Showcasing research from the Nanoregulatory Laboratory of Drug Discovery and Development Department, Italian Institute of Technology, Genoa, Italy.

Dissolution test for risk assessment of nanoparticles: a pilot study

Human ingestion of silver nanoparticles is simulated by an *in vitro* digestive assay under dynamic conditions. Nanoparticles quite completely dissolve in ionic soluble complexes and smaller nanostructures, which remain bound in the intestinal environment following the excretion pathway of faeces (typical of in bulk material). The test quantifies few percentages of bioavailable ionic species that enter the systemic circulation through the blood. These predicted amounts were validated by *in vivo* pharmacokinetics. The work describes the biotransformation of silver nanoparticles in the digestive tract and experimentally demonstrates the read-across principle between nanoforms and the (non-nano) parental form.

ROYAL SOCIETY OF **CHEMISTRY**
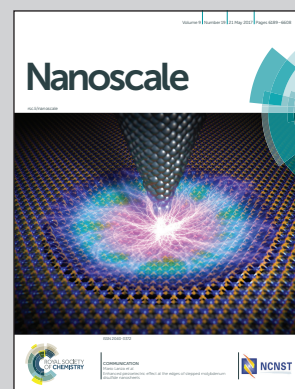
rsc.li/nanoscale

Registered charity number: 207890

Dissolution test for risk assessment of nanoparticles: a pilot study†

Pasquale Bove,[a] Maria Ada Malvindi,[b] Sachin Sayaji Kote,[a] Rosalia Bertorelli,[a] Maria Summa[a] and Stefania Sabella*[a]

Worldwide efforts are currently trying to produce effective risk assessment models for orally ingested nanoparticles. These tests should provide quantitative information on the bioaccessibility and bioavailability of products of biotransformation, such as dissolved ionic species and/or aggregates. *In vitro* dissolution tests might be useful for nanoparticle risk assessment, because of their potential to quantitatively monitor the changes of specific properties (*e.g.*, dissolution, agglomeration, *etc.*), which are critical factors linked to bioaccessibility/bioavailability. Unfortunately, the technological advancement of such tools is currently hampered by the complexity and evolving nature of nanoparticle properties that are strongly influenced by the environment and are often difficult to trace in a standardized manner. Hence, the test's success depends on its ability to quantify such properties using standardized experimental conditions to mimic reality as closely as possible. Here we applied an *in vitro* dissolution test to quantify the dissolution of silver nanoparticles under dynamic conditions, which likely occur in human digestion, providing a clear description of the bioaccessible ionic species (free and matrix bound ions or soluble silver organic or inorganic complexes) occurring during the different digestion phases. We demonstrated the test feasibility using a multi-technique approach and following pre-standardized operational procedures to allow for a comprehensive description of the process as a whole. Moreover, this can favour data reliability for benchmarking. Finally, we showed how the estimated values of the bioaccessible ionic species relate to absorption and excretion parameters, as measured *in vivo*. The outcomes presented in this work highlight the potential regulatory role of the dissolution test for orally ingested nanoparticles and, although preliminary, experimentally demonstrate the regulatory oriented "read-across" principle.

Introduction

With the increasing industrial production and use of commercial goods containing nanomaterials, human oral exposure to nanoparticles (NPs) is likely.[1] This makes urgent the establishment of feasible risk assessment models that take into account the quantification of the oral bioaccessibility of NPs and/or of their biotransformation products (as for instance dissolved ionic species) under conditions simulating human ingestion. Their quantification is necessary to enable a relationship with NP bioavailability, as measured *in vivo*.[1–3] In the case of regulation of food contaminants and/or drugs, bioavailability represents the portion of molecular species (drugs or contaminants) released from the ingested initial amount that reaches the systemic circulation.[4,5] As such, bioavailability is a key factor with a direct impact on regulatory parameters, such as the No-Observed-Adverse-Effect Level (NOAEL) and Tolerable Daily Intake (TDI).[6–8] *In vitro* dissolution tests are used worldwide to measure the bioaccessibility of drugs/contaminants, a property considered to be a prerequisite for molecular duodenal absorption and, hence, an indicator *in vitro* of molecule bioavailability *in vivo*.[5,9] Dissolution tests might be useful analytical tools for the regulatory assessment of orally ingested NPs, as they present the potentiality to quantitatively monitor the changes of extrinsic properties of NPs (*i.e.* dissolution, agglomeration, *etc.*) in simulated biological media, which are critical factors for the measurement of bioaccessibility/bioavailability.[10–12] Unfortunately, the technological advancement of such tools is currently hampered by the

[a]Istituto Italiano di Tecnologia, Drug Discovery and Development Department, Via Morego, 30–16136 Genova, Italy. E-mail: pasquale.bove@iit.it, sachin.kote@iit.it, rosalia.bertorelli@iit.it, maria.summa@iit.it, stefania.sabella@iit.it; Fax: +39 010 717 81 228; Tel: +39 010 717 81 289
[b]Istituto Italiano di Tecnologia, Center for Bio-Molecular Nanotechnologies@UniLe, Via Barsanti, 73010 Arnesano (Lecce), Italy. E-mail: mariada.malvindi@iit.it
†Electronic supplementary information (ESI) available. See DOI: 10.1039/c6nr08131b

complexity of these properties that are subjected to changes (due to the surrounding environment) and by the lack of standardized studies on the complete characterization of NP biotransformation under realistic conditions.[10–12] Hence, the test's success depends on its ability to quantify such properties, using experimental conditions, which are realistic and standardized as far as possible.[13] Currently, some *in vitro* digestion models using artificial matrixes simulating human digestion (*e.g.*, gastro intestinal fluid, acidic pH, food matrix) have been employed for different types of NPs, using various experimental designs that involve the static or dynamic incubation of NPs. They provide information on biotransformations that lead to changes in the NP size and alteration of colloidal stability in gastrointestinal fluids by a range of techniques.[14–21] Despite providing interesting structural information on NP aggregates, a complete characterization of the biotransformations under realistic conditions that include the quantification of dissolution and secondary unknown products (*e.g.*, ionic molecular species which, in turn, might be bioaccessible) is still missing. Moreover, the lack of standardized procedures for artificial matrix/assay preparation and techniques to measure the specific endpoints (dissolution, aggregation, *etc.*) represents another limiting factor. This latter point strongly hampers the successful development of dissolution tests as well as the production of reliable data, in principle, useful for benchmarking. International bodies, such as EC, ECHA, EPA, ISO and many others argue that both points should be addressed.[22–26] Finally, to our knowledge, the quantified fractions of bioaccessible ionic species that are possibly derived from dissolution (*e.g.*, free or bound to matrix ions) by the *in vitro* test have never been compared to *in vivo* absorption and excretion values.

As a backdrop to the need for establishing comprehensive characterisation of NP biotransformation, this work attempts to focus on the possible regulatory role of the dissolution test when assessed with NPs. We first performed the complete characterisation of reference silver nanoparticles (AgNPs) under simulated human digestive conditions, mimicking oral exposure by applying a dynamic *in vitro* digestion assay, previously developed for quantifying the bioaccessibility of food contaminants.[4,5] AgNPs were selected as a case study due to their high industrial production and consumer use (food industry, packaging, personal care products, *etc.*).[1–3] We applied a multi-technique based approach and, where possible, followed standard operating procedures (published or under submission through the European project, NANoREG)[27] and a reference material (NM300k) to foster future benchmarking. Analytical techniques were carefully selected to gain complementary information necessary to describe complex processes. Changes in the NP size, plasmon absorption, dissolution, quantification of free and bound to matrix ions, were measured as test endpoints (physical descriptors) and further analysed for a comprehensive whole process description. Finally, the estimated values of the dissolved ionic species have been compared to excretion and absorption parameters as measured by *in vivo* studies.

Results and discussion

To study the digestion of NPs, we applied an *in vitro* dissolution test originally developed for measuring the bioaccessibility of food contaminants.[4,5] The test was slightly adapted and performed in a dynamic mode in a unique reaction tube. The assay simulates human oral digestion, accounting for salt and protein composition, pH jumps, transit times and volume changes, which typically occur in the oro-gastrointestinal tract (OGI) during food passage (Scheme 1).

As model NPs, we selected AgNPs, known as NM300k, which are extensively characterized under many conditions and through many methods.[28] These NPs were approved for the Organisation for Economic Co-operation and Development (OECD) testing program, and are used as reference materials in many EU projects in the nanoregulatory context (NANoREG, MARINA).[27,29] In other research areas (food contaminants, pharmaceuticals), dissolution tests suffer reproducibility issues and the need for harmonization and standardization of methodologies/techniques is deeply discussed.[30,31] In the field of NP characterization, this is further hampered by the fact that no consensus for basic characterization requirements of
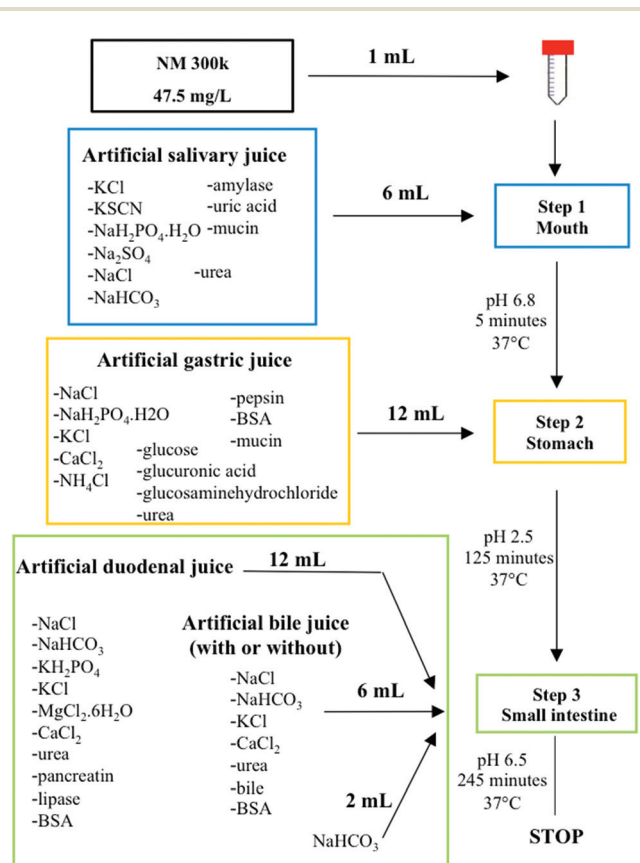
Scheme 1 Simulated oral digestive model. The scheme describes the passage of NPs along the OGI tract and the key physical conditions that they progressively experience during the digestion process (time of digestion, pH, fluid volume, juice molecule composition, NP concentration) (details in the Methods section).

the main physical properties of NPs, even in simple solutions, has been reached so far.[26,32] Hence, we aimed to improve the data quality using, where possible, pre-Standard Operational Procedures (SOPs) developed within the European project NANoREG and an EPA protocol coupled with the use of a reference material.[27] The SOPs employed account for most of the assay steps, ranging from methods for material preparation (*i.e.*, the NANOGENOTOX protocol for NP dispersion, calibration of the probe sonicator (Jensen *et al.*, submitted), preparation of TEM grids, preparation of digestive juices (van der Zande *et al.*, Deliverable 5.2, NANoREG submitted)) and instrument use (*i.e.*, Transmission Electron Microscopy, TEM, and Dynamic Light Scattering, DLS) (see the Methods section for details).[33,34] By this approach, a characterization dataset, including size distribution, zeta potential and UV-Vis absorption has been provided for NM300k immediately after dispersion in the dispersant solution (Fig. 1). Consistent with the NP datasheet, we observed the presence of primary NPs of 15 ± 5 nm (Fig. 1A) by TEM, whereas DLS measurements detected larger NPs of 40 ± 3 nm (Fig. 1B). This larger size might be explained in terms of hydrodynamic diameters along with the presence of small NP aggregates in the solution. Our results are in line with a previous study on the same NPs.[35] The zeta potential, under these dispersant conditions, was −24 ± 5 mV (Fig. 1C) while the typical SPR peak was centred around 412 nm in the UV-Vis spectral analysis (Fig. 1D). Note that the CTRL shows also a second peak at about 450 nm possibly indicative of small aggregates in a poly-dispersed mixture. Dissolution of NM300k was calculated in dispersion medium after the application of the dispersion protocol by Ultrafiltration/Inductively Coupled Plasma-Adsorption Emission Spectroscopy (UF/ICP-AES), finding a percentage of ions released with respect to the total silver content of nanoparticles, corresponding to about 0.1%.

Following characterization in the dispersion medium, NM300k were tested by the *in vitro* digestion test, according to the steps reported in Scheme 1.[4,5] The biotransformation of NM300k during digestion is a complex and dynamic process, and the occurrence of agglomeration/aggregation and dissolution may be envisaged.[11] Hence, to provide quantitative information on the structural modifications occurring to NPs during digestion, we applied a multi-technique approach involving TEM, DLS, UV-Vis, and UF/ICP-AES. Each of these techniques provides a unique advantage to gain complementary information, necessary for a comprehensive description of the process as whole. Fig. 2 shows the characterization dataset of NM300k in simulated salivary juice. A TEM method developed by De Temmerman *et al.* and used as the basis for the SOP developed by NANoREG, was applied herein, to provide a semiquantitative, statistical analysis of the NP size distribution within the complex matrix (Fig. 2A and B).[34] Data analysis was conducted on more than 1000 particles per image on approximately 100 selected images. Results indicate that, upon simulated salivary juice exposure, NPs maintain their primary size with a peak size distribution of 21 ± 18 nm, although agglomerated structures in the range of 40–70 nm are also detectable. Although DLS measurements in complex matrices only provide a qualitative representation of the particle size distribution in the solution (due to the presence of big aggregates masking smaller particles),[36] DLS spectra report a peak size distribution, which goes from 14 ± 3 nm to 120 ± 4 nm (indicating the formation of agglomerates from primary NPs). The peak at 14 nm may represent micelle structures of the stabilizers present within the solution, as also reported by another study,
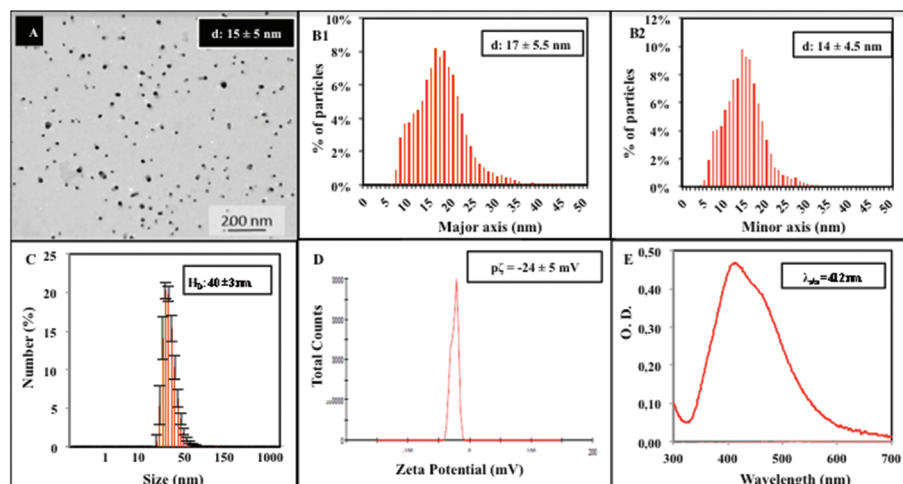
Fig. 1 Characterization dataset of NM300k in dispersion medium. (A) Representative TEM image of NM300k (scale bar 200 nm). Values given are the standard deviation averaged over at least 1000 nanoparticles analysed; (B) % of particle size distribution *vs.* major and minor axes; size has been calculated based on NP circularity (values between 0.5 and 1) and averaged on the two measured values to obtain the final size. (C) DLS histograms are based on the number−size peak distribution (PdI: 0.626); the measurements are the average of at least 10 runs, each containing 15 sub-measurements (PdI: polydispersion index); (D) zeta potential measurements are the average of at least 10 runs. (E) UV-Vis spectrum after the dispersion protocol. All measurements (except UV-Vis) were conducted following SOPs as developed within the NANoREG project (see the Methods section).
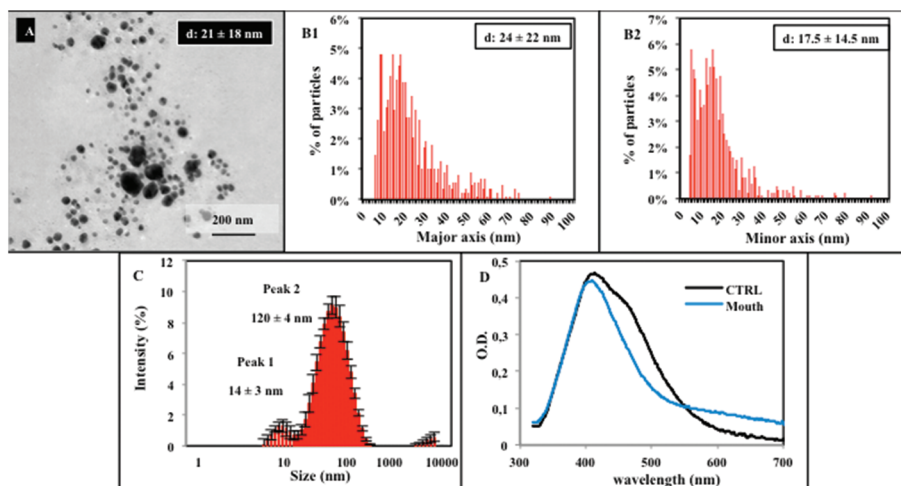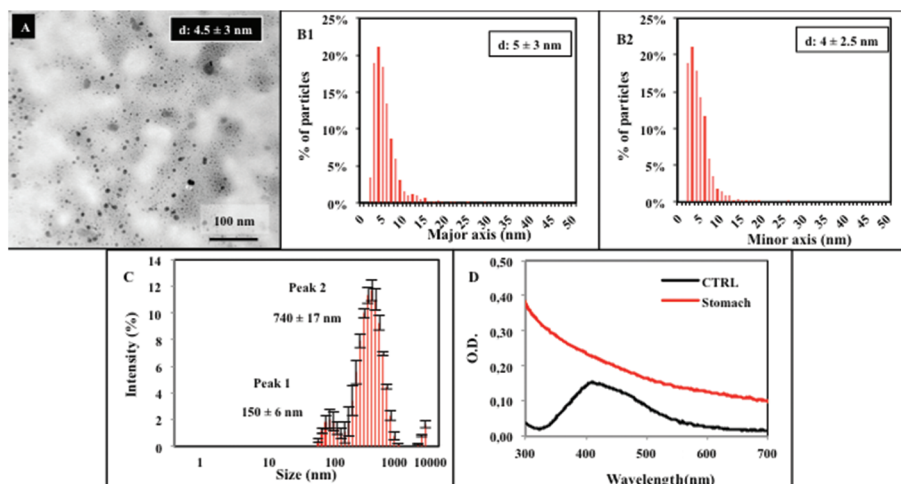
Fig. 2 NM300k digestion by the *in vitro* dissolution test (step 1: artificial salivary juice). (A) Representative TEM image of NM300k in simulated saliva juice (scale bar 200 nm). Values given are standard deviation averaged over at least 1000 nanoparticles analysed; (B) % of particle size distribution *vs.* major and minor axes; size has been calculated based on NP circularity (values between 0.5 and 1) and averaged on the two measured values to obtain the final size. (C) DLS intensity-based size peak distribution of NM300k; measurements are the average of at least 10 runs, each containing 15 sub-measurements; (D) UV-Vis spectra analysis. All measurements (except UV-Vis) were conducted following SOPs as developed within the NANoREG project (see the Methods section).

which utilised NM300k.[35] In the presence of saliva, UV-Vis analysis shows only the absorption peak at 412 nm, possibly due to a stabilizing effect of the size of primary NPs in the solution (possibly due to the protein corona) along with a broad band covering the 550–650 nanometer region (typical indicator of newly formed agglomerates),[37] thus confirming that the solution is a polydispersed mixture made of primary nanoparticles and agglomerates/aggregates (Fig. 2D). Overall, the data indicate that no dissolution occurs at this digestion

step, but rather, agglomeration/aggregation phenomena take place.

Along the passage under stomach simulating conditions (step 2), TEM analysis of the resulting mixture shows a quite different situation, evidencing a high degree of particle dissolution and the presence of smaller NPs, with a mean diameter of about 5 ± 3 nm. Some big agglomerates, also detected by DLS (Fig. 3A–C), are present. Their formation might be due to the contribution of the organic matrix. Additional represen-

Fig. 3 NM300k digestion by the *in vitro* dissolution test (step 2: artificial gastric juice). (A) Representative TEM image of NM300k after transit from simulated saliva juice into stomach simulating conditions (scale bar 100 nm). Values given are standard deviation averaged over at least 1000 nanoparticles analysed; (B) % of particle size distribution *vs.* major and minor axes; size has been calculated based on NP circularity (values between 0.5 and 1) and averaged on the two measured values to obtain the final size; (C) DLS intensity-based size peak distribution of NM300k; measurements are the average of at least 10 runs, each containing 15 sub-measurements; (D) UV-vis spectrum shows a broad and non-specific absorption band. All measurements (except UV-vis) were taken following SOPs as developed within the NANoREG project (see the Methods section).

tative TEM images are reported in the ESI (Fig. S1†). From TEM data, we calculated an approximate dissolution of about 95% for NM300k. The NP dissolution is also confirmed by the UV-Vis spectra displaying the absence of the peak at 412 nm, replaced by a broad absorption band (Fig. 3D).

UF is a separation technique commonly applied to evaluate protein–ion (drug) interactions.[38,39] UF was employed here to discriminate and quantify the fraction of free dissolved ions and/or silver organic or inorganic soluble complexes (which may pass the filter through the eluate) *vs.* the bound ions (that, remain within the filter retentate due to matrix binding/interaction). Hence, the digested solution (sampled after 2 hour stomach incubation) was subjected to UF. The resulting supernatant was measured by ICP-AES, and returned a value of dissolved silver free ions and/or silver soluble complexes of *ca.* 19% (Fig. 4) (absolute silver ion concentration is reported in Fig. S2†). Such a value represents the free ionic fraction (free silver ions and/or their soluble complexes) that does not bind the matrix under these specific environmental conditions, whereas the remaining 81% fraction corresponds to ions bound to the matrix (*i.e.*, proteins, AgCl precipitates, *etc.*), in line with TEM and UV-Vis data. This was also verified by control experiments, in which a standard ion solution at the same concentration (corresponding to completely dissolved NM300k) was digested by the *in vitro* dissolution test. Also in this latter case, results show similar proportions, with the supernatant containing an amount of ions or soluble silver complexes corresponding to about 18% of the total ions initially present in the solution before UF (Fig. 4 and ESI Fig. S2†), while the remaining 82% interacted with the matrix and were retained within the filter. Furthermore control experiments to evaluate the nonspecific loss of ions due to filter adhesion or matrix fouling were performed using AgNO$_3$ solu-

tions.[40] Results indicated an average recovery of silver >88%, suggesting that the loss of ions can therefore be regarded as negligible (not shown). These results were also in agreement with van der Zande *et al.*, showing no specific adhesion of silver solutions to a 3 kDa filter.[35] Results also indicate that, in the stomach environment, the dissolution of NPs is almost complete (Fig. 3A, B and D). Overall, these data suggest that silver ions, after being released by NPs, mostly interact with the matrix through various processes, including silver chloride formation or chelation to sulphur groups of proteins, and only a small fraction (*ca.* 20%) is present as free ions or soluble inorganic and organic complexes.[14,18,35,41,42] Such a complex mixture undergoes further biotransformation. Upon reaching the intestine compartment (Fig. 5) (step 3), TEM and DLS evidence significantly aggregated large structures (Fig. 5A–C) and a small population of NPs with the size ranging from 5 to 50–60 nm. Under these conditions UV-Vis spectra are affected by interference of the strong absorption of bile salts in the visible region of the spectrum. We thus performed the dissolution test also in their absence, however no specific signal for inorganic AgNPs was detectable (Fig. 5D) under these experimental conditions. The presence of the nanosized forms suggests that the intestinal environment favours the formation of nano Ag+ salts (although in lower proportion with respect to the initial amount of NPs). This is in line with recent findings, both *in vitro* and *in vivo*, showing the presence of nanosized silver salts (containing sulphur and chloride) in cells/tissues upon treatments with AgNPs or silver salts (*e.g.*, AgNO$_3$ or AgAc).[18,35,41] Furthermore, similar nanostructures were also reported to occur in the skin of argyria patients.[18,35,41,43]

Examined together, these results suggest that the dissolution in the intestinal site of NM300k is maintained in a similar state to that of the stomach environment, but the dissolved fraction of free ions and/or silver soluble complexes (as quantified by UF/ICP-AES) is reduced to about 2% (thus 98% of silver ions are in the form of either silver nanosized salts or matrix-bound species) (Fig. 4 and calibration experiments in Fig. S2†).

In conclusion, our data indicate that NM300k do not maintain their primary properties along the passage through the OGI tract, undergoing an almost complete dissolution (Fig. 2–6). In particular, when orally digested, NPs begin to partially agglomerate in the salivary compartment (Fig. 6). Upon reaching the stomach compartment, the specific environmental conditions (molecular composition and acidic pH) prime the dissolution (see below). This process is almost total (90–95%) with a small fraction of dissolved free ions and/or silver soluble complexes (*ca.* 19%), whereas the remaining 81% are matrix-bound ions and salt precipitates. As the bolus passes to the small intestine, the free fraction is reduced to about 2%, while the bound fraction increases up to 98%. Within this fraction, we observed the presence of aggregates as well as nanosized particles of different organic natures.[18,35,41]

Interestingly, we measured the amount of dissolved molecular oxygen in the digestive compartments, finding values corresponding to 8.63, 8.50 and 7.40 mg L^{-1} in the saliva,
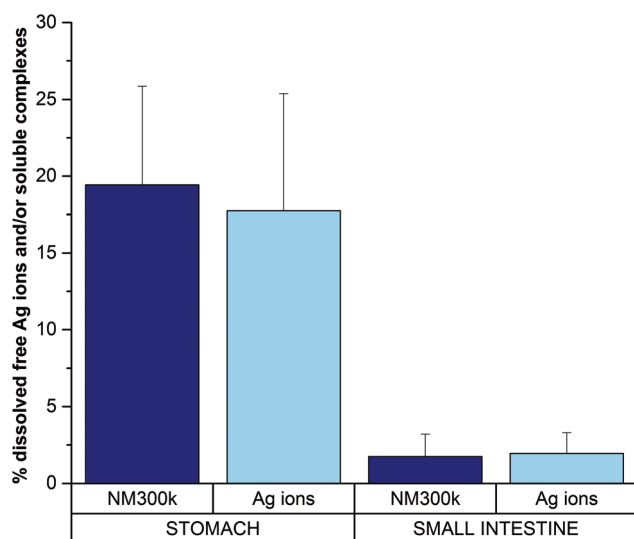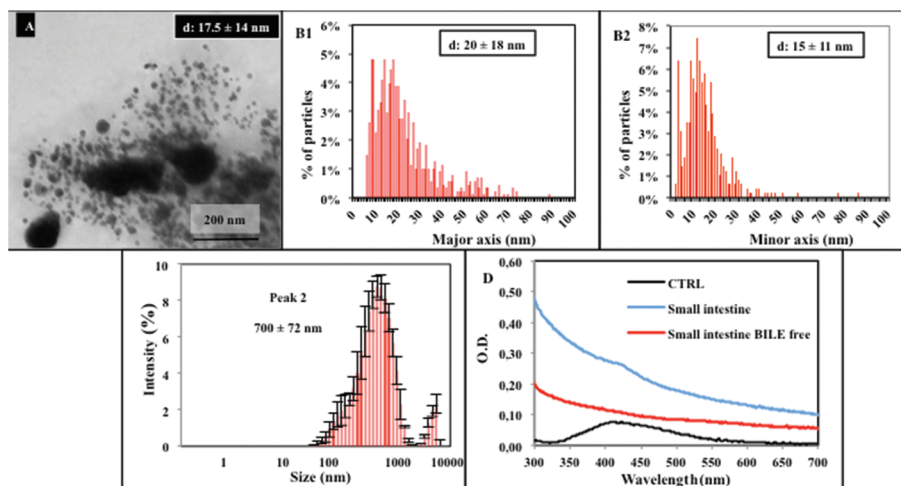

Fig. 4 % of dissolved silver free ions and/or silver soluble complexes during NP digestion in stomach and intestine compartments (silver ions at equal concentrations are used as the internal control in calibration experiments).

Fig. 5 NM300k digestion by the *in vitro* dissolution test (step 3: artificial intestine juice). (A) Representative TEM image of NM300k after transit from simulated stomach juice into intestinal simulating conditions (scale bar 200 nm). Values given are the standard deviation averaged over at least 1000 nanoparticles analysed; (B) % of particle size distribution *vs.* major and minor axes; size has been calculated based on NP circularity (values between 0.5 and 1) and averaged on the two measured values to obtain the final size; (C) DLS intensity-based size peak distribution of NM300k; measurements are the average of at least 10 runs, each containing 15 sub-measurements; (D) UV-Vis spectrum shows the disappearance of the plasmon peak at 412 nm and the presence of a broad and a specific absorption. All measurements (except UV-Vis) were taken following SOPs as developed within the NANoREG project (see the Methods section).
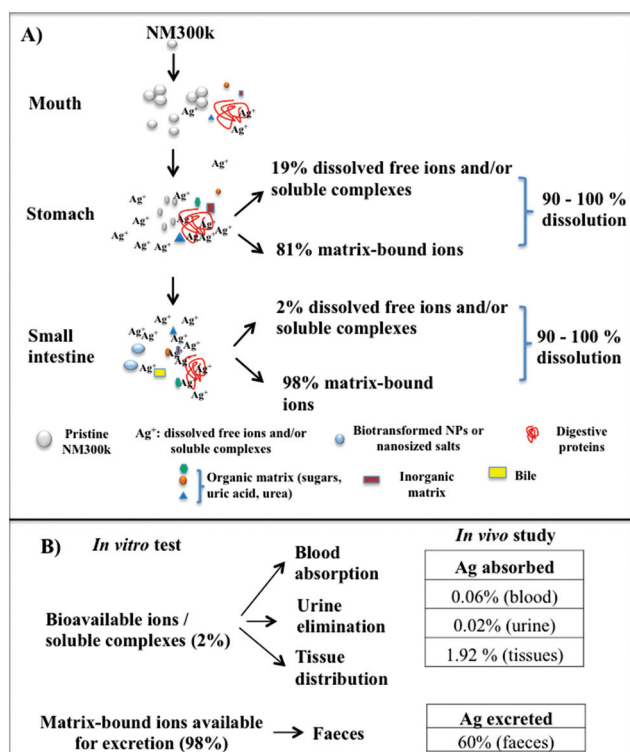
Fig. 6 (A) Cartoon of the *in vitro* dissolution of NM300k and quantification of the biotransformation products (free and matrix-bound ions); (B) absorption and excretion values of silver ions as predicted *in vitro* and measured by *in vivo* experiments.

stomach and intestine, respectively. From the obtained values, it seems that they are quite equally distributed through the OGI tract. Hence, as the NP dissolution is mostly observed

under simulating stomach conditions, it seems that a cooperative oxidation process, which requires the presence of both dissolved molecular oxygen and protons is required. This confirms, also for the case of digestive juices, the well-established theory of oxygen-proton mediated dissolution, previously developed by Liu & Hurt (to demonstrate the mechanism, they used citrate capped colloidal silver nanoparticles in water and in simulating organic matrixes of sea water).[42]

This *in vitro* dissolution test, with its indication on both NP behaviour and bioavailability parameters, may be relevant for the risk assessment of AgNPs. It represents a useful analytical tool for two reasons: first, it demonstrates that the majority of the initial NPs are dissolved as ions after oral digestion, thus the NM300k are no longer in a nanoform. Hence the NP exposure levels are likely to be not very different from those generated by their corresponding saline form. This is crucial because, to establish risk assessment and related risk exposure levels for AgNPs, we could directly refer to the established exposure threshold levels of silver ions (*e.g.*, TDI and NOAEL) as measured for humans, by applying read-across principles.[7,44] Secondly, since these ions appear to be mostly bound to the matrix, their excretion will likely follow the same excretion pathway (through bile and faeces) typically found for the silver saline form in humans and animals (rats, mice, dogs, monkeys), which interestingly had been found to be around 94–99% of the total ingested silver.[45,46] The remaining ions will then be available for translocation, though only a limited fraction is expected to reach systemic circulation for further tissue distribution, metabolism and urine elimination (ADME). The levels of absorption for orally administered silver have been described to be low, ranging from 0.4–10% in animals, results which change with the species considered.

Moreover, in the case of AgNPs, the bioavailability was found to be even lower based on high faecal excretion and lower absolute silver levels found in organs.[35,41]

Hence, based on these regulatory driven observations, we verified our read-across based hypothesis, by checking the excretion and absorption values *in vivo* (Fig. 6B). Mice were exposed to NM300k for 28 days, by oral gavage, with a daily dose corresponding to 25 µg per mouse (1 mg per kg b.w.). Note that this dosage is about 0.4 fold lower than the NOAEL (No-Observed-Adverse-Effect Level) level and 40 folds higher than the human TDI (Tolerable Daily Intake).[7] The silver content in faeces and urine was measured by ICP-AES after collection of the samples at 7 or 21 days, whereas blood was collected at the end of the treatment to reduce animal testing (details in the Methods section) (Fig. S3†). The measured silver ion concentration in the faeces and urine is reported as % with respect to the total daily intake per mouse in Fig. 6 and as an absolute amount in the ESI (Fig. S3†). Results show that the excreted silver ions in the faeces were estimated at about 60% (Fig. 6B). This value is slightly lower than that predicted by the test. However, measurements of silver in the faeces are actually challenging and may provide only qualitative information, as also reported in previous studies showing that 60–99% of the administered silver dose is recovered in faeces.[31,44,47] For the remaining bioavailable fraction (2%), we found a silver content in the blood corresponding to about 0.06% of the total daily intake and 0.02% excreted by urine. Hence, the remaining bioavailable fraction (about 1.9%) is likely to be adsorbed and distributed in the tissues, as reported by other studies *in vivo*.[31,41]

In conclusion, the values of dissolved free ionic species possibly bioaccessible (*i.e.* 98% bound to the matrix and 2% in the form of free ions and/or silver soluble complexes) as estimated by the *in vitro* test, have been compared to excretion and absorption parameters measured by *in vivo* studies, finding that most of the ions bound to the matrix are excreted through faeces (or remain deposited onto the intestinal wall) and a very small portion is absorbed and distributed through blood, urine and tissues.

The presented dissolution test and the obtained outcomes can improve the process of risk assessment (RA) for NPs. Currently the RA for ingested NPs requires quantitative information on solubility and/or durability and/or bio persistence of NPs, as these are the key means required by risk assessors to carry out adequate risk assessment and address its paradigm (identification and characterization of a hazard in relation to exposure threshold levels).[25] The test also enables substance identification that is one of the bases for the preparation of a substance dossier in the framework of REACH.[50] Finally, by providing a quantitative description of bioaccessible soluble species, when associated with *in vivo* pharmacokinetic data (ADME), the test may become predictive and mechanistic. On the other side, many regulatory frameworks increasingly ask for the development of grouping approaches dedicated to nanomaterials. Grouping tools usually compare conventional substances in a common group based on their structural simi-

larities. Hence, endpoint-specific effects of an unknown substance may be derived from the well-known endpoint effects of other substances within the group.[51–54] Similarly, in its standardized form, the dissolution test can be a useful tool for grouping NPs on the bases of their functionalities and/or properties influenced by the environment, and for the case of highly dissolving NPs, the possible toxic effects along with threshold exposure levels (for instance NOAEL and TDI) can be derived by comparison with the parent material.

Conclusions

In conclusion, the biotransformation of NPs in biological matrixes, which mimic human oral exposure, is a complex process influenced by many properties. Such factors relate not only to the properties of NPs (size, aggregation state, solubility, *etc.*), but also to the properties of the selected matrixes (pH, temperature, ionic strength) as well as to the assay set-up. Thus, the application of a multi-technique approach and pre-standardized procedures may be helpful. We applied TEM, UV-Vis, DLS and UF/ICP-AES to harness unique assets from each technique to gain a complementarity spread of information. This provided us with a clear and quantitative description of the AgNP dissolution process, using an *in vitro* oral digestive assay, which employs human digestive simulating matrixes and dynamic conditions. Results indicate that >90% dissolution of silver nanoparticles is already complete when NPs transit through the stomach. However, the resulting ions are not all bioavailable, as many of them bind to the digestive matrices in different forms (bound to matrix, aggregates, nanosized organic salts) (98%), while only 2% are free dissolved ions and/or silver soluble complexes bioaccessible for duodenal absorption. These estimated values have been supported by *in vivo* studies that, although preliminary, show that most of the NPs are present in the faeces, thus suggesting that the excretion behaviour of NPs is comparable to that of the corresponding saline form, and that it may be derived by read-across principles. Further studies (*e.g.*, inter-laboratory comparison) are needed to further validate these findings.

Methods

Dispersion of NM300k and calibration of the probe sonicator

NM300k were obtained from the repository list of the European Commission Joint Research Centre (JRC). They are AgNPs with a declared nominal size of about 20 nm. The received vials contain an aqueous nano-silver dispersion, including 10.16% w/w of the metal, 7% w/w of the stabilizing agent ammonium nitrate, 4% w/w polyoxyethylene glycerol trioleate and 4% w/w polyoxyethylene sorbitan monolaurate. The NM300k stock solution was diluted at the experimental concentrations, according to the NANOGENOTOX dispersion protocol, that foresees sonication of AgNPs using a probe

sonicator.[33] Briefly, before starting the experimental session, the probe sonicator (Sonics Vibracell VC750) equipped with a 13 mm probe was calibrated by using a calorimetric procedure, according to the NANoREG "SOP for probe-sonicator calibration of delivered acoustic power and de-agglomeration efficiency for *in vitro* and *in vivo* toxicological testing" with the aim of ensuring inter-laboratory harmonization of the dispersion conditions (Jensen *et al.*, submitted). As resulted from the calorimetric calibration, the sonication parameters, necessary to deliver the same acoustic power as that used in the NANOGENOTOX protocol, were 20% amplitude and 8 minutes and 30 seconds duration of sonication. These calculated parameters were confirmed by testing the de-agglomeration efficiency on the reference material NM200 and analysing the dispersion efficiency by DLS, according to the "SOP for measurement of hydrodynamic Size-Distribution and Dispersion Stability by Dynamic Light Scattering (DLS)" provided by NANoREG (Jensen *et al.*, submitted) (see also below). After calibrating the probe sonicator, 151.2 mg of the NM300k viscous material was weighed into a glass scintillation vial and 6 mL of the dispersion medium was added to obtain the operative concentration of 2.56 g L^{-1}. The sonicator was then set to the conditions outlined above during calibration (20% of amplitude) and NPs were subjected to sonication for 8 minutes and 30 seconds. A stock dispersion of NM300k was then diluted in dispersion medium at the working concentration of 47.5 mg L^{-1}. The size distribution of the solution was then checked immediately by DLS (see below).

Dynamic light scattering (DLS) analysis

Dynamic light scattering (DLS) measurements were performed on a Zetasizer Nano ZS90 (Malvern, USA) equipped with a 4.0 mW HeNe laser operating at 633 nm and an avalanche photodiode detector. Measurements (10 runs) were made at 25 °C using disposable polystyrene cuvettes. The refractive index (R_i) and the adsorption index (R_{abs}) were 0.180 and 0.010 respectively, according to the SOP for measurement of hydrodynamic Size-Distribution and Dispersion Stability by Dynamic Light Scattering (DLS) provided by NANoREG (Jensen *et al.*, submitted). The size of NM300k was monitored at time zero in the dispersion medium at the concentration of 47.5 mg L^{-1} and after 5, 125 and 245 minutes in the presence of matrices simulating the mouth, stomach and small intestine at the final concentration of 1.2 mg L^{-1}.

Artificial human digestive juices

The digestion of NPs was monitored by an *in vitro* dynamic model, elaborated from the method described by Versantvoort *et al.* (see below) and following a SOP developed within NANoREG (van der Zande *et al.* NANoREG, Deliverable 5.2 submitted).[5] Briefly, artificial juices (or defined in the text also as matrixes) were prepared by mixing salt solutions, organic compounds and proteins under pH conditions similar to those present in the human digestive compartments (mouth, stomach and small intestine).[5] All digestive fluids were pre-

pared on the first day, by combining each required ingredients at fixed concentrations and pH values to a final volume of 1 L (Table 1 and TS1†). The juices were incubated overnight at room temperature. On the second day (assay day), the juices were pre-heated to 37 °C for at least two hours.

The saliva juice was prepared with ions, organic compounds and proteins as reported in Table 1, adjusting the pH to 6.8 ± 0.1 with 37% HCl.

For the gastric juice, ions, carbohydrates, urea and proteins were mixed following the scheme in Table 2 (and TS2†) and adjusting the pH at 1.3 ± 0.1 with 37% HCl.

Finally, the small intestine juice was employed with both duodenal (pH 8.1 ± 0.1) and bile (pH 8.2 ± 0.1) solutions added to a solution of 84.7 g L^{-1} sodium bicarbonate (Table 3 and TS3†). All chemicals were purchased from Sigma Aldrich.

Table 1 Composition of the artificial salivary juice used in the *in vitro* digestion model

Mouth

Ions	Final concentration (g L^{-1})
KCl	0.90
KSCN	0.20
$NaH_2PO_4 \cdot H_2O$	1.02
Na_2SO_4	0.57
NaCl	0.30
$NaHCO_3$	1.70
Organic compounds	**Final concentration (g L^{-1})**
Urea	0.20
Uric acid	0.01
Proteins	**Final concentration (g L^{-1})**
Amylase	0.29
Mucin	0.02
Dissolved molecular oxygen	**Final concentration (mg L^{-1})**
O_2	8.63

Table 2 Composition of the artificial gastric juice used in the *in vitro* digestion model

Stomach

Ions	Final concentration (g L^{-1})
NaCl	2.75
$NaH_2PO_4 \cdot H_2O$	0.31
KCl	0.82
$CaCl_2$	0.30
NH_4Cl	0.31
Organic compounds	**Final concentration (g L^{-1})**
Glucose	0.65
Glucuronic acid	0.02
Glucosaminehydrochloride	0.33
Urea	0.09
Proteins	**Final concentration (g L^{-1})**
BSA	1.00
Pepsin	2.5
Mucin	3.00
Dissolved molecular oxygen	**Final concentration (mg L^{-1})**
O_2	8.50

Table 3 Composition of the artificial small intestine juice used in the *in vitro* digestion model

Small intestine			
Duodenum		**Bile**	
Chemicals	**Final concentration (g L^{-1})**	**Chemicals**	**Final concentration (g L^{-1})**
NaCl	7.00	NaCl	5.30
NaHCO$_3$	3.38	NaHCO$_3$	5.80
KH$_2$PO$_4$	0.08	KCl	0.38
KCl	0.56	CaCl$_2$	0.16
MgCl$_2$·6H$_2$O	0.05		
CaCl$_2$	0.15		
Organic compounds	**Final concentration (g L^{-1})**	**Organic compounds**	**Final concentration (g L^{-1})**
Urea	0.02	Urea	0.25
Proteins	**Final concentration (g L^{-1})**	**Proteins**	**Final concentration (g L^{-1})**
BSA	1.00	BSA	1.80
Pancreatin	9.00	Bile	30.00
Lipase	1.50		
Dissolved molecular oxygen		**Final concentration (g L^{-1})**	
O$_2$		7.40	

Dissolved molecular oxygen was measured in the digestive juices under conditions of air saturated water, at room temperature, by means of a dissolved oxygen probe (YSI Pro ODO).

Dynamic human *in vitro* digestion

The dynamic human *in vitro* digestion was employed to assess the dissolution of NM300k following a SOP developed within NANoREG (van der Zande *et al.* NANoREG, Deliverable 5.2 submitted) and the method described by Versantvoort *et al.*[5] 1 mL of the NP suspension at a working concentration of 47.5 mg L^{-1} or a correspondent saline solution (47.5 mg L^{-1}) was injected into a 50 mL tube and then the different juices (see above) were added in a temporal sequence that simulates the transit of food bolus along the OGI tract. The mouth compartment was achieved, mixing 6 mL of salivary juice at pH 6.8 with 1 mL of both NP suspension and ICP silver standard ions and processing one of the three distinct batches. By shaking at 37 °C, after 5 minutes of incubation, the mouth sample was analyzed by DLS, TEM, UV-Vis and UF/ICP-AES.

The other two batches were employed to continue the transit into the subsequent sector that is the stomach. Therefore they were added to 12 mL of gastric juice, brought at pH 2.5 ± 0.5 with 1 M NaOH and incubated for further 120 minutes at 37 °C. After that, one of the two stomach samples was processed for the multi-technique based characterization.

The last batch was employed to simulate digestion in the small intestine, adding to it 12 mL of duodenal fluid, 6 mL of bile salts and 2 mL of 84.7 g L^{-1} sodium bicarbonate and adjusting the pH at 6.5 ± 0.5 with 37% HCl. The shaking was stopped after further 120 minutes of incubation.

Each compartment was carried out in triplicate. 7 independent experiments were carried out.

Transmission electron microscopy (TEM) analysis

The NP size and morphology in the dispersion medium and synthetic digestive juices were evaluated by TEM. Images were recorded using a JEOL JEM 1011 microscope operating at an accelerating voltage of 100 kV. TEM samples were prepared by dropping a dilute solution of nanoparticles in water on carbon-coated copper grids (Carbon 400 Mesh Cu). The performance of the TEM was evaluated using a calibration sample. TEM micrographs were recorded, following a standardized procedure developed in the EU project NANoREG.[34] Briefly, TEM specimens were prepared using the grid on drop method by contacting a carbon-coated, 400 mesh carbon grid (Agar Scientific, Essex, England), pre-treated with 1% alcian blue (Sigma, USA) with 10 µL of the diluted dispersion. The grid is left in contact with the sample for 10 minutes before it is blotted to remove the excess of sample and left to air-dry at room temperature. Grids were stored in a Petri-dish on a piece of filter paper until analysis. All the steps for TEM sample preparation were performed under a chemical hood. The repeatability (within one-day variability) and intermediate precision (day-to-day variability) are estimated as follows: three (different) vials are analysed on three days within one week; on each day, two TEM specimens are prepared from one vial. From each TEM specimen, micrographs of ten regions on the grid are recorded and analysed. At least 500 particles were analysed per specimen.

Digital micrographs were taken randomly at a magnification of 12 000, pixel size 0.56 nm and micrograph size 1511.61 × 1500.36 (nm). Micrographs were analysed using the Image J software (National Institutes of Health, USA). For each micrograph manual grey-scale thresholding was performed. All images are binarised and a separate particle filter was applied to separate touching particles. Particles touching the bottom and right and left sides of the image were manually rejected. After image analysis, only particles with circularity between 0.5–1 were defined as single primary particles. From each NM300k specimen, a representative micrograph and the corresponding annotated micrograph were selected.

Ultraviolet-visible (UV-Vis) analysis

A UV-Vis spectrophotometer (UV-3600 Shimadzu) was used to monitor the plasmon peak of NM300k. The starting suspension at 47.5 mg L^{-1} was read to identify both the size and concentration related intensity of the peak at 412 nm. Further, UV-Vis measurements were performed on the digested juices obtained after incubation of NM300k for 5, 125 and 245 minutes in the mouth, stomach and small intestine simulating juices. After incubation, the resulting solutions were pelleted and the resulting pellets were re-suspended in MilliQ water (18.2 MΩ cm, at 25 °C) to obtain the final NP concentration in each digestive compartment.

UF/ICP-AES analysis

Standard silver solutions (ICP standard) or NM300k (47.5 mg L^{-1}) were digested using the *in vitro* digestion assay and the resulting solutions were then passed through the filtration membrane (Amikon 3 kDa filter membranes, Merck Millipore) according to the manufacturer's instructions. The flow-throughs contain free ions only, whereas the matrix (with proteins) and the matrix–ion complex were retained by the filter. For control experiments, standard solutions of AgNO$_3$ with or without 0.05% of albumin (as employed for the NANOGENOTOX protocol), at increasing NP concentrations, were also passed through the filtration membrane (Amikon 3 kDa filter membranes, Merck Millipore) according to the manufacturer's instructions (data not shown).

Flowthroughs were dissolved in 0.5 mL of 70% HNO$_3$ (Sigma Aldrich) and diluted to 5 mL with MilliQ water to be then quantified by ICP-AES. Elemental analysis was carried out by inductively coupled plasma atomic emission spectroscopy (ICP-AES, Agilent 720/730 spectrometer). ICP calibration standards were used to construct a multipoint standard curve covering the range of analyte concentrations possibly present in the samples. Data that fell in this concentration range were considered valid.

The total silver content was determined from whole blood, urine and faeces. Urine and faeces were collected at 7 or 21 days and 0.5 g was weighed for digestion following the EPA 200.8 1994 protocol.[48] The collected faeces correspond to an approximation of a total mass of faeces of 1.5 g per day and urine to 1 mL per day. Blood (about 2.5 mL per day in a mouse) was collected through the tail vein at the end of 28 days and digested by weighing ~1 g in 1 mL of nitric acid 70%, followed by a microwave treatment (temperature: 175 °C, pressure: 400, power: 300). Extra care has been taken during the collection of whole blood samples used for total silver measurements to avoid the loss of silver during the separation process. The silver content was measured by ICP-AES as reported above.

Animal studies

Male CD1 mice (22–24 g, Charles River, Calco, Italy) were used. Animals were group-housed in ventilated cages and had free access to food and water. They were allowed to acclimatize under a 12-hour light/dark cycle (lights on at 8:00 am) at a controlled temperature of (21 ± 1) °C and relative humidity of (55 ± 10%) for one week before starting the experiments. Mice were then randomly divided into 2 groups (*n* = 5), and the treated group was exposed daily to NM300k 1 mg kg^{-1} for 28 days *via* oral gavage. The animals were fasted two hours before the oral treatment. All procedures performed were carried out in accordance with the guidelines established by the European Communities Council Directive (Directive 2010/63/EU of 22 September 2010) and approved by the National Council on Animal Care of the Italian Ministry of Health.[49] All efforts were made to minimize animal suffering and to use the minimal number of animals required to produce reliable results.

Abbreviations

NPs	Nanoparticles
AgNPs	Silver nanoparticles
OGI tract	Oro-gastro-intestinal tract
TEM	Transmission electron microscopy
DLS	Dynamic light scattering
UV-Vis:	Ultraviolet-visible
UF	Ultrafiltration
ICP-AES	Inductively coupled plasma-adsorption emission spectroscopy
NOAEL	No-observed-adverse-effect level
TDI	Tolerable daily intake
EC	European Commission
ECHA	European Chemicals Agency
EPA	United States Environmental Protection Agency
ISO	International Organization for Standardization
OECD	Organisation for Economic Co-operation and Development
SOP	Standard Operational Procedure
CTRL	Control
PdI	Polydispersity index
ADME	Absorption, distribution, metabolism and excretion
JRC	European Commission Joint Research Centre
RA	Risk assessment.

Acknowledgements

References

1 M. E. J. Pronk, *et al.*, *Nanomaterials under REACH: Nanosilver as a case study*, *RIVM Report 601780003*, 2009.

2 D. M. Mitrano, S. Motellier, S. Clavaguera and B. Nowack, Review of nanomaterial aging and transformations through the life cycle of nano-enhanced products, *Environ. Int.*, 2015, **77**, 132–147, DOI: 10.1016/j.envint.2015.01.013.

3 Q. Chaudhry, *et al.*, Applications and implications of nano-technologies for the food sector, *Food Addit. Contam., Part A*, 2008, **25**, 241–258, DOI: 10.1080/02652030701744538.

4 A. G. Oomen, *et al.*, Development of an *in vitro* digestion model for estimating the bioaccessibility of soil contaminants, *Arch. Environ. Contam. Toxicol.*, 2003, **44**, 281–287, DOI: 10.1007/s00244-002-1278-0.

5 C. H. M. Versantvoort, A. G. Oomen, E. Van de Kamp, C. J. Rompelberg and A. J. Sips, Applicability of an *in vitro* digestion model in assessing the bioaccessibility of myco-toxins from food, *Food Chem. Toxicol.*, 2005, **43**, 31–40, DOI: 10.1016/j.fct.2004.08.007.

6 R. R. Rodriguez, N. T. Basta, S. W. Casteel and L. W. Pace, An *in vitro* gastrointestinal method to estimate bioavailable arsenic in contaminated soils and solid media, *Environ. Sci. Technol.*, 1999, **33**, 642–649, DOI: 10.1021/es980631h.

7 N. Hadrup and H. R. Lam, Oral toxicity of silver ions, silver nanoparticles and colloidal silver – A review, *Regul. Toxicol. Pharmacol.*, 2014, **68**, 1–7, DOI: 10.1016/j.yrtph.2013.11.002.

8 E. Nielsen, G. Ostergaard and J. T. Larsen, *Toxicological risk assessment of chemicals: A practical guide*, Informa Healthcare, 2008.

9 J.-M. Cardot, E. Beyssac and M. Alric, *In vitro – in vivo* corre-lation: Importance of dissolution in IVIVC, *Dissolution Technol.*, 2007, **14**, 15–19, DOI: 10.14227/DT140107P15.

10 A. E. Nel, *et al.*, Where are we heading in nanotechnology environmental health and safety and materials characteriz-ation?, *ACS Nano*, 2015, **9**, 5627–5630, DOI: 10.1021/acsnano.5b03496.

11 V. Stone, *et al.*, ITS-NANO - prioritising nanosafety research to develop a stakeholder driven intelligent testing strategy, *Part. Fibre Toxicol.*, 2014, **11**, 9, DOI: 10.1186/1743-8977-11-9.

12 J. J. Scott-Fordsmand, *et al.*, A unified framework for nano-safety is needed, *Nano Today*, 2014, **9**, 546–549.

13 S. K. Misra, A. Dybowska, D. Berhanu, S. N. Luoma and E. Valsami-Jones, The complexity of nanoparticle dis-solution and its importance in nanotoxicological studies, *Sci. Total Environ.*, 2012, **438**, 225–232, DOI: 10.1016/j.scitotenv.2012.08.066.

14 J. L. Axson, *et al.*, Rapid kinetics of size and pH-dependent dissolution and aggregation of silver nanoparticles in simulated gastric fluid, *J. Phys. Chem. C*, 2015, **119**, 20632–20641, DOI: 10.1021/acs.jpcc.5b03634.

15 K. R. Rogers, *et al.*, Alterations in physical state of silver nanoparticles exposed to synthetic human stomach fluid, *Sci. Total Environ.*, 2012, **420**, 334–339, DOI: 10.1016/j.scitotenv.2012.01.044.

16 P. N. Wiecinski, *et al.*, Gastrointestinal biodurability of engineered nanoparticles: Development of an *in vitro* assay, *Nanotoxicology*, 2009, **3**, 202–214, DOI: 10.1080/17435390902859556.

17 A. P. Walczak, *et al.*, Behaviour of silver nanoparticles and silver ions in an *in vitro* human gastrointestinal digestion model, *Nanotoxicology*, 2013, **7**, 1198–1210, DOI: 10.3109/17435390.2012.726382.

18 R. Peters, *et al.*, Presence of nano-sized silica during *in vitro* digestion of foods containing silica as a food additive, *ACS Nano*, 2012, **6**, 2441–2451, DOI: 10.1021/nn204728k.

19 L. Böhmert, *et al.*, Analytically monitored digestion of silver nanoparticles and their toxicity on human intestinal cells, *Nanotoxicology*, 2014, **8**, 631–642, DOI: 10.3109/17435390.2013.815284.

20 D. Lichtenstein, *et al.*, Impact of food components during *in vitro* digestion of silver nanoparticles on cellular uptake and cytotoxicity in intestinal cells, *Biol. Chem.*, 2015, **396**, 1255–1264, DOI: 10.1515/hsz-2015-0145.

21 R. Lei, *et al.*, Integrated metabolomic analysis of the nano-sized copper particle-induced hepatotoxicity and nephro-toxicity in rats: a rapid *in vivo* screening method for nano-toxicity, *Toxicol. Appl. Pharmacol.*, 2008, **232**, 292–301, DOI: 10.1016/j.taap.2008.06.026.

22 European Chemicals Agency, Guidance on Information Requirements and Chemical Safety Assessment, Chapter R.7a: Endpoint specific guidance, 2015.

23 European Chemicals Agency, Guidance on information requirements and chemical safety assessment, Appendix R7-1 Recommendations for nanomaterials applicable to Chapter R7a – Endpoint specific guidance, 2012.

24 Organisation for economic co-operation and development, Environment directorate joint meeting of the chemicals committee and the working party on chemicals, pesticides and biotechnology, 2009.

25 EFSA, Guidance on the risk assessment of the application of nanoscience and nanotechnologies in the food and feed chain, *EFSA J.*, 2011, **9**, 2140–2176, DOI: 10.2903/j.efsa.2011.2140.

26 E. Valsami-Jones and I. Lynch, How safe are nanomaterials?, *Science*, 2015, **350**, 388–389, DOI: 10.1126/science.aac9505.

27 NANoREG – A common European approach to the regulat-ory testing of nanomaterials. http://www.nanoreg.eu/.

28 C. L. Klein, *et al.*, NM-series of representative manufactured nanomaterials. NM-300 silver, Characterisation, stability, homogeneity, 2011, 1–86, DOI: 10.2788/23079.

29 MARINA – Managing risks of nanomaterials. http://www.marina-fp7.eu/.

30 E. Jantratid, N. Janssen, C. Reppas and J. B. Dressman, Dissolution media simulating conditions in the proximal human gastrointestinal tract: an update, *Pharm. Res.*, 2008, **25**, 1663–1676, DOI: 10.1007/s11095-008-9569-4.

31 V. Gray, *et al.*, The science of USP 1 and 2 dissolution: present challenges and future relevance, *Pharm. Res.*, 2009, **26**, 1289–1302, DOI: 10.1007/s11095-008-9822-x.

32 S. Buck, Solving reproducibility, *Science*, 2015, **348**, 1403, DOI: 10.1126/science.aac8041.

33 NANOGENOTOX. http://www.nanogenotox.eu/files/PDF/Deliverables/nanogenotox20deliverable203_wp4_20dispersion20protocol.pdf.

34 P.-J. De Temmerman, *et al.*, Measurement uncertainties of size, shape, and surface measurements using transmission electron microscopy of near-monodisperse, near-spherical nanoparticles, *J. Nanopart. Res.*, 2014, **16**, 2177, DOI: 10.1007/s11051-013-2177-1.

35 M. van der Zande, *et al.*, Distribution, elimination, and toxicity of silver nanoparticles and silver ions in rats after 28-day oral exposure, *ACS Nano*, 2012, **6**, 7427–7442, DOI: 10.1021/nn302649p.

36 E. Tomaszewska, *et al.*, Detection limits of DLS and UV-Vis spectroscopy in characterization of polydisperse nano-particles colloids, *J. Nanomater.*, 2013, **2013**, 313081, DOI: 10.1155/2013/313081.

37 K. Aslan, J. R. Lakowicz and C. D. Geddes, Plasmon light scattering in biology and medicine: new sensing approaches, visions and perspectives, *Curr. Opin. Chem. Biol.*, 2005, **9**, 538–544, DOI: 10.1016/j.cbpa.2005.08.021.

38 M. Quaglia, *et al.*, Search of ligands for the amyloidogenic protein beta2-microglobulin by capillary electrophoresis and other techniques, *Electrophoresis*, 2005, **26**, 4055–4063, DOI: 10.1002/elps.200500313.

39 J. Sommer-Knudsen and A. Bacic, A micro-scale method for determining relative metal-binding affinities of proteins, *Mol. Biotechnol.*, 1997, **8**, 215–218, DOI: 10.1007/BF02760774.

40 I. H. Huisman, P. Prádanos and A. Hernández, The effect of protein–protein and protein–membrane interactions on membrane fouling in ultrafiltration, *J. Membr. Sci.*, 2000, **179**, 79–90, DOI: 10.1016/S0376-7388(00)00501-9.

41 K. Loeschner, *et al.*, Distribution of silver in rats following 28 days of repeated oral exposure to silver nanoparticles or silver acetate, *Part. Fibre Toxicol.*, 2011, **8**(18), 1–14, DOI: 10.1186/1743-8977-8-18.

42 J. Liu and R. H. Hurt, Ion release kinetics and particle persistence in aqueous nano-silver colloids, *Environ. Sci. Technol.*, 2010, **44**, 2169–2175, DOI: 10.1021/es9035557.

43 D. Massi and M. Santucci, Human generalized argyria: a submicroscopic and X-ray spectroscopic study, *Ultrastruct. Pathol.*, 1998, **22**, 47–53, DOI: 10.3109/01913129809032257.

44 A. G. Oomen, *et al.*, Grouping and read-across approaches for risk assessment of nanomaterials, *J. Environ. Res. Public Health*, 2015, **12**, 13415–13434, DOI: 10.3390/ijerph121013415.

45 B. W. East, K. Boddy, E. D. Williams, D. Macintyre and A. L. Mclay, Silver retention, total body silver and tissue silver concentrations in argyria associated with exposure to an anti-smoking remedy containing silver acetate, *Clin. Exp. Dermatol.*, 1980, **5**, 305–311, DOI: 10.1111/j.1365-2230.1980.tb01708.x.

46 J. E. Furchner, C. R. Richmond and G. A. Drake, Comparative metabolism of radionuclides in mammals-IV. Retention of silver-110m in the mouse, rat, monkey, and dog, *Health Phys.*, 1968, **15**, 505–514, DOI: 10.1097/00004032-196812000-00005.

47 I. L. Bergin, *et al.*, Effects of particle size and coating on toxicologic parameters, fecal elimination kinetics and tissue distribution of acutely ingested silver nanoparticles in a mouse model, *Nanotoxicology*, 2016, **10**, 352–360, DOI: 10.3109/17435390.2015.

48 United States Enviromental Protection Agency, Method 200.8, Revision 5.4: Determination of Trace Elements in waters and wastes by inductively coupled plasma – mass spectrometry, 1994.

49 DIRECTIVE 2010/63/EU of the European Parliament and of the Council of 22 September 2010 on the protection of animals used for scientific purposes, *Official Journal of the European Union*, 2010.

50 J. H. E. Arts, *et al.*, A critical appraisal of existing concepts for the grouping of nanomaterials, *Regul. Toxicol. Pharmacol.*, 2014, **70**, 492–506, DOI: 10.1016/j.yrtph.2014.07.025.

51 ECHA, European Chemicals Agency, Assessment of Read-across in REACH, 2012a.

52 ECHA, European Chemicals Agency, Grouping of Substances and Read-across Approach. Part I. Introductory note, 2013.

53 ECHA, European Chemicals Agency, Human health and environmental exposure assessment and risk characterization of nanomaterials. Best practice for REACH registrants, 2013.

54 OECD, Organisation for economic co-operation and development, Guidance on grouping of chemicals, second edition, Series on Testing and Assessment, 194, 2014.